

# FRACTURE OF WOOD COMPOSITES AND WOOD-ADHESIVE JOINTS: A COMPARATIVE REVIEW

*Michael P.C. Conrad*

Graduate Research Assistant  
Department of Metals and Materials Engineering

*Gregory D. Smith*<sup>†</sup>

Assistant Professor  
Department of Wood Science

and

*Göran Fernlund*

Assistant Professor  
Department of Metals and Materials Engineering  
The University of British Columbia  
Vancouver, BC Canada V6T 1Z4

(Received April 2002)

## ABSTRACT

This paper presents a comparative review of the literature on fracture of wood composites and wood-adhesive joints. Wood-adhesive joints are two or more adherends joined with resin in a specific geometry. Wood composites can be considered an amalgamation of wood-adhesive joints, and the effect of geometry, adherends, and resin on fracture toughness for wood-adhesive joints is similar to that of wood composites. Parameters that have similar effects on the two systems are: slenderness ratio, a purely geometrical consideration; adherend surface preparation; and bond-line uniformity, where ideally, the bond-line is self-similar along the entire length. Applicability of fracture mechanics is also demonstrated as models based on the concept of intrinsic flaws have been found to adequately predict fracture behavior of these composites.

**Keywords:** Fracture mechanics, wood/adhesive joints, wood composites, resin dispersion, resin distribution, oriented strandboard.

## INTRODUCTION

Over the past decades, the use of wood composites has increased. While the literature on fracture of solid wood is extensive, limited research has been undertaken on fracture of wood composites. The fracture behavior of solid wood is important when studying wood composites as wood composites are identical to solid wood up to the cellular level, with the only difference being that at larger scales, the wood-adhesive bonds add further complexity to the wood composite not present in solid wood. Wood composites can be considered an

amalgamation of wood-adhesive joints. As one moves to larger and larger furnish, from particles to strands to veneer, only the length to thickness ratio of the furnish changes, and each composite is essentially a series of adhesive joints. Therefore, an examination of the structural adhesive joint literature, which is related to the furnish-resin (meso) scale of wood composites, will allow greater understanding of the behavior of wood composites at the macroscopic scale.

The literature can be divided into wood-adhesive research and wood-composite research, with the majority of studies concentrating on either the geometry of the joint or composite,

---

<sup>†</sup> Member of SWST and corresponding author.

effects associated with the adherend, or effects associated with the adhesive. Table 1 lists the wood-adhesive joint fracture toughness geometries, adhesives, species, and effects examined in the literature. Table 2 lists the relevant literature for wood composites.

The resin system used in wood composites is typically phenol-formaldehyde (Barnes 2000, 2001), but isocyanate resins have also been studied (Lei and Wilson 1979, 1980; Youngquist et al. 1987; Kamke et al. 1996; Furuno et al. 1983).

Literature on fracture of wood composites relating to joint geometry, adherend characteristics, and resin will now be discussed in more detail. The literature will be discussed in relation to the behavior of structural adhesive joints, and the findings summarized. Note that this is not an exhaustive but a select review that compares reported fracture behavior of wood composites and wood-adhesive joints.

#### SPECIMEN GEOMETRY

The strength and fracture toughness of wood composites can be more easily interpreted by drawing on the large body of research on structural adhesive joint behavior. Examples of common structural adhesive joints are shown in Fig. 1. Geometric parameters examined in the literature include the effect of lamination or veneer thickness and lap length.

An examination of the adhesive lap and strap joint literature reveals that a reduction in lamination thickness reduces both the shear and peel stresses at the end of the bonded overlap (Tong and Steven 1999). For wood-adhesive joints, it has similarly been found that a decrease in lamination thickness leads to an increase in fracture toughness and failure stress (Leicester 1973; Komatsu et al. 1976; Walsh et al. 1973; Leicester and Bunker 1969; Jung and Murphy 1983; River et al. 1989; Scott et al. 1992). The effect of lamination thickness on failure stress is shown in Fig. 2, with sufficiently thin laminations having fracture loads similar to that of defect-free wood.

At the macroscopic scale, similar observations are made. Lei and Wilson (1979) show that there is a reduction in fracture toughness with increasing veneer thickness, a result also corroborated by Jung and Murphy (1983). Lei and Wilson also found that for LVL constructed with very thin veneers, 0.8 mm (1/32 in.), the directionality of solid wood disappears for the RL, TL, TR, or RT crack directions, and therefore crack direction has no effect on the fracture toughness. This finding should be applicable to other wood composites since the thickness of the veneer is similar to that of OSB strands. Thus, the fracture toughness of OSB should not be affected by the orthotropic nature of solid wood.

Of the two remaining dimensions for adhesive joints, width and length, the one typically studied is lap length. Results of Leicester (1974), Komatsu et al. (1976), and Walsh et al. (1973) indicate that the failure load of lap and strap joints increases with lap length. However, as shown in Fig. 3, increasing the overlap length leads to diminishing returns and the normalized failure load plateaus above a characteristic length, for a given system. The plot of normalized failure load,  $P\alpha/2Y$ , versus normalized lap length,  $0.5\alpha L$ , in Fig. 3 allows a dimensionless comparison of load and lap length.

Komatsu (1984) examined Mode III fracture toughness by bonding lap shear samples at varying angles and loading the samples in compression. The ratio of Mode II to Mode III is a function of the angle between the adherends with a significant Mode II component at large angles (pure Mode II at 180°). The  $G_{IIIc}$  value decreased as the angle increased from 90° to 180°. The fracture pattern also changed with lap angle. At low lap angles (90° and 120°), fracture was simple and brittle, occurring through fracture in rolling shear at the glue lines. At angles of 150° and above, fracture was more complex, with some samples failing within the wooden members themselves.

For modelling purposes, it is often easier to describe the properties of wood composites in

TABLE 1. Wood-adhesive fracture specimen geometries, adhesives, species, and effects examined in the literature.

| Specimen geometry                       | Resin                     |                                     |                 |                  |                                     |                |               |
|---|---------------------------|-------------------------------------|-----------------|------------------|-------------------------------------|----------------|---------------|
|   | C*                        | E                                   | P               | PR               | R                                   | RF             | UF            |
| Single Lap                              |                           |                                     |                 |                  |                                     |                |               |
| Double Lap                              |                           | LC, LT, LC: (2)                     | Sh**, BL†: (1)‡ |                  |                                     |                |               |
|   |                           | P, LC: (3)                          |                 |                  |                                     |                |               |
| Butt Double Strap                       | P, Bi, Q, Bk, LT, LC: (4) | LC, LT, LC: (2)                     |                 |                  |                                     |                | P, LT: (5, 6) |
| Butt                                    |                           | Elk, Cp, Sla, BT, D, T, BL, SC: (7) |                 | DE, LT, SC: (8)  | Elk, Cp, Sla, BT, D, T, BL, SC: (7) |                | P, DF: (9)    |
| Compact Tension (CT)                    | P, BL: (10)               |                                     |                 |                  |                                     | C, M, BL: (11) |               |
| Double Cantilever Beam (DCB)            |                           |                                     | YP, BL: (12)    |                  |                                     |                | Bi: (13)      |
| Contoured Double Cantilever Beam (CDCB) |                           |                                     |                 |                  |                                     |                |               |
|   |                           |                                     |                 | A: (14)          |                                     |                |               |
|   |                           |                                     |                 | M: (14–20)       |                                     |                |               |
|   |                           |                                     |                 | Bi, LT: (21)     |                                     |                |               |
|   |                           |                                     |                 | BL: (15, 17)     |                                     |                |               |
|   |                           |                                     |                 | SC: (16, 18, 20) |                                     |                |               |
| Four Point Bend                         |                           |                                     |                 |                  |                                     |                | P, DF: (9)    |

\* Resins: C = casein, E = epoxy, P = phenolic, PR = phenol-resorcinol, R = resorcinol, RF = resorcinol-formaldehyde, UF = urea-formaldehyde.

\*\* Species: A = Aspen, Bi = Birch, Bk = Blackwood, BT = Brown Terminalia, C = Cedar, Cp = Camptopserma, D = Dillenia, DF = Douglas Fir, Elk = East Indian Kauri, LC = Lawson Cypress, M = Maple, P = Pine, Q = Quandong, Sh = Shinanoki, Sla = Solomon Island Albizia, T = Taun, YP = Yellow Poplar.

† Effects: BL = bond-line, LC = lap characteristics, LT = lamination thickness, SC = surface characteristics.

‡ Authors: 1 = Shimizu and Okuma 1981; 2 = Komatsu et al. 1976; 3 = Komatsu 1984; 4 = Walsh et al. 1973; 5 = Leicester, 1973; 6 = Leicester and Bunker, 1969; 7 = Sasaki et al. 1973; 8 = Jung and Murphy 1983; 9 = Smith and Penney 1980; 10 = White 1976; 11 = White and Green 1980; 12 = Gagliano and Frazier 2001; 13 = River et al. 1989; 14 = River and Okkonen 1993; 15 = Ebewe et al. 1979; 16 = Ebewe et al. 1980; 17 = Ebewe et al. 1982; 18 = Ebewe et al. 1986a; 19 = Ebewe et al. 1986b; 20 = Mijovic and Koutsky 1979; 21 = Scott et al. 1992.

TABLE 2. Wood composite fracture toughness specimen geometries, species, and effects examined in the literature.

| Specimen geometry                       | Composite                        |  |   |                    |                                 |
|---|----------------------------------|--|---|--------------------|---------------------------------|
|   | Glued laminated timbers (Glulam) | Laminated veneer lumber (LVL)                | Oriented strand board (OSB)   | Particleboard (PB) | Medium density fiberboard (MDF) |
| Three Point Bend                        | DF*, D**; (1)†                   | DE, C, S, L, D: (3)<br>DE, BL, $\rho$ : (5)  | C, BL, $\rho$ : (2)<br>DF: (5)<br>A: (6, 7)<br>Ad, Bi, C, P: (7)<br>$\rho$ : (5)<br>BL: (5, 8, 9)   | DF: (10)           | U, D: (4)                       |
| Compact Tension (CT)                    |                                  |  |   |                    |                                 |
| Internal Bond (IB)                      |                                  |  |   |                    |                                 |
| Compact Tension Shear (CTS)             |                                  | DF: (12)<br>BL, $\rho$ (5)<br>D, LT: (5, 12) | DF: (5, 13)<br>A: (6)<br>$\rho$ : (5, 13)<br>BL: (5, 8)<br>U: (14)<br>A: (7, 15)<br>Bi: (7, 16)<br>DF: (16)<br>Ad, C, P: (7)<br>BL: (15)<br>LC, LT: (16)<br>U, TS: (17) | DF: (10)           | U, D: (11)                      |
| Single Edge Notch (SEN)                 |                                  |  |   |                    |                                 |
| Contoured Double Cantilever Beam (CDCB) |                                  |  |   |                    |                                 |
| Tension                                 |                                  |  |   | P: (14)            |                                 |
| Unknown                                 |                                  |  |   |                    |                                 |

\* Species: A = Aspen, Ad = Alder, Bi = Birch, C = Cedar, DF = Douglas Fir, L = Larch, P = Pine, S = Spruce, U = unknown.

\*\* Effects: BL = bond-line, D = defects, LC = lap characteristics, LT = lamination thickness,  $\rho$  = density, TS = tensile strength.

† Authors: 1 = Murphy 1986; 2 = Barnes 2000; 3 = Mihashi and Hoshino 1989; 4 = Sato 1988a; 5 = Lei and Wilson 1980; 6 = Youngquist et al. 1987; 7 = Higgins 1990; 8 = Kamke et al. 1996; 9 = Furuno et al. 1983; 10 = Ilciewicz and Wilson 1981; 11 = Sato 1988b; 12 = Lei and Wilson 1979; 13 = Lei and Wilson 1981; 14 = River and Okkonen 1993; 15 = Laufenberg 1984; 16 = Barnes 2001; 17 = Simpson 1977.

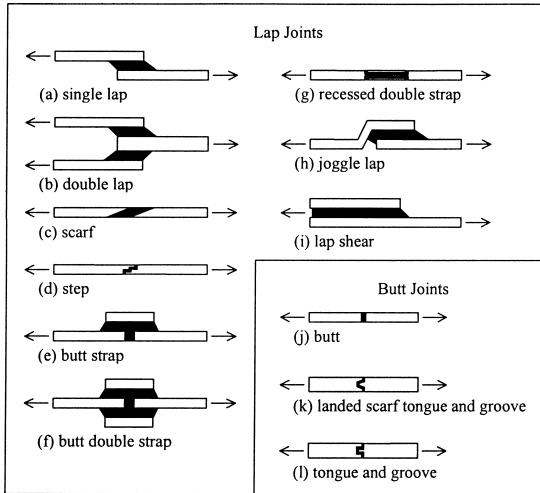


FIG. 1. Some common structural bonded lap joints (a–i) and butt joints (j–l). (Tong and Steven 1999)

terms of the ratio of furnish length to thickness. This ratio is referred to as the slenderness ratio. Barnes (2001), Eqs. (1) and (2), and Simpson (1977), Eqs. (3) to (5), developed models based on the inherent properties of wood and the slenderness ratio. Barnes uses a modified Hankinson equation, whereas Simpson's model accounts for the shear strength of the adhesive used. (It should be noted that the symbols for the variables within these and subsequent equations have been changed for ease of comparison.)

#### Barnes Model:

$$\sigma_R = \frac{\sigma_{\parallel} \times \sigma_{\perp}}{\sigma_{\parallel} \sin^n[\arctan(2t_b/l)] + \sigma_{\perp} \cos^n[\arctan(2t_b/l)]}, \quad (1)$$

$$t_b = t_a \times \left( \frac{\rho_a}{\rho_b} \right), \quad (2)$$

where  $\sigma_R$  is the resultant strength (psi),  $\sigma_{\parallel}$ , the strength parallel to the grain (psi),  $\sigma_{\perp}$ , the strength perpendicular to the grain (psi),  $n$ , the experimentally determined coefficient (0.9 to 1.5),  $l$ , the length of strand (in),  $t_a$ , the initial strand thickness (in),  $t_b$ , the *in situ* strand thickness (in),  $\rho_a$ , the initial wood density (lb/ft<sup>3</sup>), and  $\rho_b$ , the product wood density (lb/ft<sup>3</sup>).

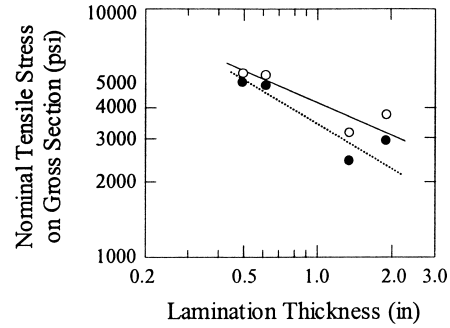


FIG. 2. Effect of lamination thickness on failure load for laminated pine containing butt joints. ○ = stress at ultimate load (psi), ● = stress at fracture (psi). Adapted from Leicester (1973).

#### Simpson Model:

$$\sigma_R = \frac{\sigma_w(r + k)}{r + ku}, \quad (3)$$

$$r = \frac{l}{t}, \quad (4)$$

$$u = \frac{\sigma_w}{\tau}, \quad (5)$$

where  $\sigma_R$  is the tensile strength of the OSB,  $\sigma_w$ , the tensile strength of the strand in the direction of orientation,  $\tau$ , the shear strength of the adhesive bond between flakes,  $r$ , the slenderness ratio,  $l$ , the flake length,  $t$ , the flake thickness, and  $k$ , the proportionality constant relating the forces for tensile and shear failure

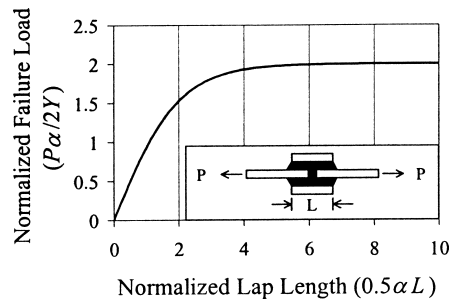


FIG. 3. Effect of lap length on failure load for a double strap butt joint where  $P$  = failure load,  $\alpha$  = f(geometry and material properties),  $Y$  = maximum allowable shear stress,  $L$  = lap length. Adapted from Tong and Steven (1999).

of the flakes to the number of strands that fail by each method (assumed to be 1).

Both models predict that at higher slenderness ratios the strength properties: modulus of elasticity (MOE) and modulus of rupture (MOR) in the Barnes model, and tensile strength in the Simpson model, increase. Increasing the slenderness ratio of the furnish is analogous to moving from OSB to Parallam™. This supports the concept of a wood composite being an amalgamation of wood-adhesive joints, as the trends of increasing failure load and stiffness with decreasing thickness and increasing length are also seen at the wood-adhesive scale. However, the Simpson model has only been compared qualitatively to data in the literature, as the author states that it would be difficult to test quantitatively.

As has been shown, models based on wood-adhesive joint geometry have been used to predict the strength of wood composites. Models based on fracture mechanics and intrinsic flaws have also been proposed. Ilcewicz and Wilson (1981) studied the fracture mechanics of particleboard using a nonlocal theory. Unlike theories based on continuum mechanics, which considers only the behavior at a point (locally), nonlocal theories take into account the behavior of a region when predicting failure. The results from Ilcewicz and Wilson (1981) show that the fracture toughness of particleboard can be predicted by Eqs. (6) and (7), which includes the intrinsic strength, intrinsic flaw size, and a characteristic dimension of the material. For the specific example modelled by Ilcewicz and Wilson, particleboards with a specific gravity of 0.70, this characteristic dimension is equal to the particle thickness. Increased particle thickness at this specific gravity gives increased fracture toughness.

$$K_{Ic} = \sigma_{IB} \sqrt{a_o} Y(a_o/W), \quad (6)$$

$$\sigma_{IB}^2 a_o = \frac{\lambda}{2k^2} \sigma_c^2, \quad (7)$$

where  $K_{Ic}$  is the Mode I fracture toughness (psi-in<sup>1/2</sup>),  $\sigma_{IB}$ , the internal bond strength (psi),

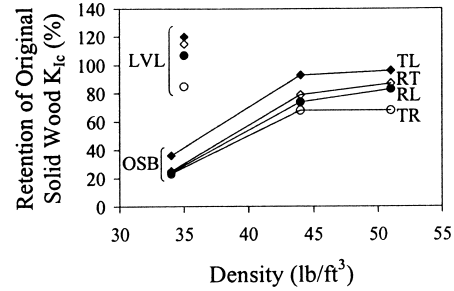


FIG. 4. Effect of board density on Mode I fracture toughness (resin spread rate = 1.350 lb/1000 ft²). Adapted from Lei and Wilson (1980).

$a_o$ , the intrinsic flaw size (in),  $Y(a_o/W)$ , the fracture toughness geometry factor,  $W$ , the width of the specimen (in),  $\lambda$ , the characteristic dimension of the material, particle thickness (in),  $\sigma_c$ , the intrinsic strength (psi), and  $k$ , the stress concentration factor equal to 0.73.

Applicability of the intrinsic flaw concept for wood composites is confirmed by the work of Lei and Wilson (1980, 1981), who studied the fracture toughness of oriented flakeboard in the TL, RT, RL, and TR directions. A TL flakeboard is equivalent to solid wood with the crack propagating in the TL direction that has been cut into flakes and re-assembled. Lei and Wilson found that the fracture toughness is affected by interflake void size and board density and is unaffected by direction and the amount of resin applied to the flake. The frequency of interflake voids reflects the uniformity of the bond-line, with the voids themselves acting as sites for crack initiation. It is assumed that the size of interflake voids will decrease with increasing board density and that LVL represents perfectly bonded OSB, e.g., OSB with no interflake voids as the bond-line is continuous rather than formed of discrete spots. Therefore, the fracture toughness of LVL can be taken as an upper bound to that of OSB. Thus, one would expect fracture toughness to decrease as the number of interflake voids increases in agreement with work by Lei and Wilson (1980), as shown in Fig. 4.

Lei and Wilson (1981) proposed a model for the prediction of fracture toughness of ori-

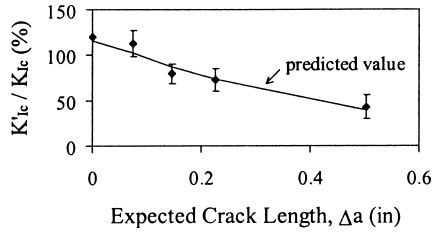


FIG. 5. Predicted and experimental retention of Mode I fracture toughness. Calculations for expected crack length are based on interflake void length plus nonbonded length. Adapted from Lei and Wilson (1981).

ented flakeboard that includes a term to account for the influence of interflake voids, Eqs. (8) and (9). This model assumes that an induced crack will be extended by an existing void or nonbonded region, and thus predicts the propagation fracture toughness of an established crack rather than the critical stress intensity factor required for crack initiation. Lei and Wilson have shown that fracture toughness of the panel is affected by the average size of the inherent flaws in the wood,  $\Omega$ , which is a material property, and the average void length,  $1/\mu$ , which is affected by resination and other processing parameters. They combined these in a proportionality constant,  $e^{(\Omega-1/\mu)}$ . This constant accounts for the possibility of producing a composite that has fracture toughness greater than that of clear, solid wood. One feature of the model is that it predicts fracture toughness identical to that of the solid wood when the average void length is set equal to the average inherent flaw size of solid wood. However, note that as the average inherent flaw size increases, an increase in board fracture toughness over that of solid wood is predicted given a constant void length.

$$\frac{K'_{Ic}}{K_{Ic}} = [e^{(\Omega-1/\mu)}] \frac{a^{1/2} Y\left(\frac{a}{W}\right)}{(a + \Delta a)^{1/2} Y\left(\frac{a + \Delta a}{W}\right)}, \quad (8)$$

$$\Delta a = \frac{1}{\mu} \left( \frac{\lambda}{\mu + \lambda} \right), \quad (9)$$

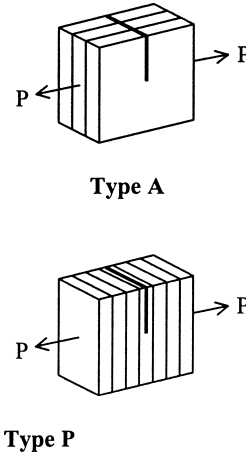


FIG. 6. Schematic of Type A, crack lies across the veneers, and Type P, crack lies parallel to the veneers, fracture geometries. Adapted from Mihashi and Hoshino (1989).

where  $K'_{Ic}$  is the fracture toughness of oriented flakeboard,  $K_{Ic}$  the fracture toughness of wood used to make strands,  $\Omega$ , the average size of inherent flaws,  $a$ , the initial crack length for an edge-notched specimen,  $\Delta a$ , the expected increase in crack length due to interflake voids,  $Y(a/W)$ , the geometry factor for edge-notched specimen,  $1/\mu$ , the average void length, and  $1/\lambda$ , the average distance between voids.

A comparison of model predictions and experimental data is shown in Fig. 5. The model predicts a  $K_{Ic}$  value equivalent to that of solid Douglas-fir at an expected crack length of 2.5 mm (0.1"), in agreement with the measured flaw size for Douglas-fir of 2.5 to 3.8 mm (0.1" to 0.15") reported by Schniewind and Lyon (1973).

Mihashi and Hoshino (1989) found that fracture mechanics, provided one used the nonlinear J-integral method, accurately predicted the experimental results on LVL. Linear fracture mechanics,  $K_{Ic}$  and  $G_{Ic}$ , underestimated the fracture toughness. Two fracture geometries were studied: one where the crack lies across (A) the veneers, and one where the crack runs parallel (P) to the veneers, both shown schematically in Fig. 6. They found



TABLE 3. *Failure mechanisms in randomly oriented strand board (Laufenberg 1984).*

| Failure pattern  | Characteristics  | Failure type (%) | Orientation of strand with respect to loading axis |
|------------------|--|------------------|--|
| Transverse/Shear | Failure along wood fiber   | 81               | 10° to 90°   |
| Rolling Shear    | Fracture perpendicular to principal stress, rotation of prismatic cross section of wood strand | 6                | 70° to 90°   |
| Tensile          | Long splintered strand end, wood fiber nearly parallel to load direction                       | 5                | <12°   |
| Disbonding       | Low strand-to-strand bond strength or high strand strength                                     | 8                | <45°   |

that the tensile strength of type A specimens was less than that of type P. However, the fracture toughness of type P specimens was less than for type A. The type A specimen is an example of crack divider geometry where the specimen acts as a series of thin plane-stress samples rather than one thick plane-strain sample (Hertzberg 1996). Since fracture toughness is higher in plane stress, the type A specimen will exhibit greater fracture toughness than type P.

However, the applicability of fracture mechanics to wood composites is not universal. Sato (1988a, b) examined the Mode I fracture toughness using a compact tension (CT) specimen and the mixed mode fracture of medium density fiberboard (MDF) and found that the fracture toughness decreased for deeper, sharper notches. Fracture toughness,  $K_{Ic}$ , was also found to increase with specimen width. Since fracture toughness is a material property, there should be no size effect associated with notch depth. Therefore, based on this, the use of linear elastic fracture mechanics is suspect in the case of MDF.

A better understanding of fracture at the macroscopic level can be obtained by examining the underlying micromechanisms of fracture. Laufenberg (1984) studied the fracture surface of OSB tested in tension, and found that the strands failed in four distinctive patterns, listed in Table 3. Examination of the table reveals that the type of failure is related to the angle of strand orientation with respect to the loading axis. This was confirmed by Barnes (2000), who found that strength de-

creased with increasing angle of the strands to the applied load for both parallel (unidirectional) and cross-angled (cross-ply) composites. The effect was less for cross-angled products due to a change in failure mode.

Laufenberg also confirmed the effect of disbond length, which includes all bond-line failures, delaminations, and any area that may not have been in contact with other flakes, inter-flake voids. The tensile strength is seen to decrease with longer disbond lengths. Since adhesive failure at the bond-line between the resin and the wood typically occurs at a lower strength than cohesive failure in either the wood or resin and longer disbond lengths correspond to an increase in the amount of bond-line failure, the tensile strength should necessarily decrease. Longer disbond lengths can also represent an increase in the size of inter-flake voids, which must decrease the tensile strength since these are zero strength regions. Laufenberg found that the orthotropic failure criteria: the maximum stress criterion, the Tsai-Hill criterion, and Hankinson's Formula, provide reasonable upper-bound estimates of the panel strength. Laufenberg attributed the deviation between predicted and measured strength to bond-line failures and recommends that the influence of bond quality should be examined using a fracture mechanics approach.

Work on specimen geometry for wood composites leads to the following conclusions. Furnish should have a high slenderness ratio (i.e., be as thin and as long as possible for a composite product with high strength). In ad-



dition, fracture mechanics predicts the behavior of wood composites with reasonable accuracy since the models for wood composites are based on intrinsic flaws within the product. Note that an increase in slenderness ratio leads to a higher surface area to volume ratio for the furnish, which will require higher resin consumption. Thus, there is a trade-off between mechanical properties and cost for the wood composite.

#### ADHEREND

Fracture behavior of wood-adhesive joints and wood composites is dependent on the fracture behavior of the solid wood as well as the surface preparation of the wood. Relevance of the fracture behavior of solid wood is most evident for glulam. Since the size of the wood component is relatively large, it behaves similarly to solid wood. In a series of studies, Murphy (1986) compared the strength reduction of notched beams to beams containing a narrow slit parallel to the long axis of the beam. It was found that slits had lower bending strengths than a notch of the same length. The magnitude of the strength reduction led Murphy to recommend that large, notched beams should be replaced with clear beams equal to the net section of unnotched material in design.

Moisture content of the wood used to form the joint also has an effect on adhesive joint performance as the fracture energy increases with decreasing moisture content, down to approximately 10% (Ebewele et al. 1986a). This is similar to solid wood where the fracture toughness passes through a maximum at approximately 6 to 8% and decreases thereafter. The difference is due to the range examined. Ebewele et al. did not study moisture contents below 10%; however, it is likely that the maximum would be found below this value. In addition, thermal effects, such as harsh drying, can compound moisture effects, and reduce the overall fracture toughness of the wood itself by introducing more and larger internal flaws.

The increase of fracture toughness and strength with increasing density for solid wood is well known. This trend has also been observed in the strength of wood composites, specifically OSB. Barnes (2000) found an increase in board properties with increased board density, and developed the following model, to predict the strength properties (MOE and MOR) of OSB:

$$F_R = F_i \left( \frac{\rho_b}{\rho_a} \right)^x, \quad (10)$$

where  $F_R$  is the resultant property, MOE or MOR (psi),  $F_i$ , the initial property, MOE or MOR (psi),  $\rho_a$ , the initial dry wood density (lb/ft<sup>3</sup>),  $\rho_b$ , the dry wood density in product (lb/ft<sup>3</sup>), and  $x$ , the exponent for the desired property (1.0 for MOE, 1.2 for MOR).

Processing of wood-adhesive joints and wood composites affects the behavior of the final product. Surface preparation of the adherends is important in the formation of an adhesive bond. Surface damage increases the discontinuity of the bond-line, thus increasing the number of internal flaws (White and Green 1980). Sasaki et al. (1973) shows that the fracture strength of a wood-adhesive bond is greatest for microtomed and planed surfaces followed by fine-sawn, rough-sawn, disk-cut (planed with a disk planer), and sanded. Each of these preparation techniques leads to increased damage of the wood fibers.

The effect of the OSB strand surface characteristics on the bond-line formed is similar to the effect of surface roughness for wood-adhesive bonds. Strands having a rough surface or containing large surface voids are more likely to trap resin and form discontinuous bonds after pressing. Strand size homogeneity is also important since increased homogeneity should, theoretically, lead to a better resin distribution (Conrad et al. 2000). Therefore, improved strand generation (i.e., reduction of the size variability between strands and the surface roughness) should improve the fracture toughness of OSB. Damage of the wood fibers can also occur through thermal degradation,

e.g., heating that results from machining with dull blades (Ebewe et al. 1986a). As above, the increased surface damage will reduce joint performance. Jung and Murphy (1983) have also shown that there is a reduction in fracture toughness with increasing veneer thickness. They speculate that as the thickness increases, there is increased damage of wood fibers.

The adherend surface will also affect the crack path in a wood-adhesive joint. There are three possible fracture paths: the crack can propagate in the wood alone, the adhesive alone, or at the wood-adhesive interface. The highest fracture energies occur in the first two cases (Ebewe et al. 1979) with a high percentage of wood failure indicating a strong adhesive bond (Ebewe et al. 1986b). The percentage of wood failure can be estimated by ASTM Practice D5266-99: Standard Practice for Estimating the Percentage of Wood Failure in Adhesive Bonded Joints (2000).

In contrast, Ebewe et al. (1980), who compared hand-sanding to machine-sanding, found that the hand-sanded surface gave higher fracture toughness than a comparable machine-sanded specimen. This was despite the fact that hand-sanding led to greater surface roughness. However, hand-sanding is done in a back-and-forth motion, whereas machine-sanding is in one direction, the direction of the grain. The back-and-forth motion of hand-sanding leads to the creation of pre-failed interfaces between fibers. These planes of weakness allow the crack to deviate from the adhesive layer and arrest the crack, thus increasing the fracture toughness.

A similar effect is seen when examining the angle the grain makes with the bond-line of the wood-adhesive specimen. Mijovic and Koutsky (1979) found that minimum fracture toughness occurs at approximately 30°. Below 30° the crack deviates into the wood, similar to the effect found by Ebewe et al. (1980) with hand-sanded substrates, giving a measurement of solid wood cohesive fracture toughness. As the grain angle is reduced from 90° to 30° there is less surface area available for resin penetration.

The studies discussed above show that the behavior of solid wood is an important factor in determining the overall behavior of wood-adhesive joints and wood composites. The effect of notches, moisture content, and density on the fracture toughness of wood composites is similar to that for solid wood. In the formation of wood-adhesive joints, surface preparation is vital to ensure that appropriate conclusions are drawn from experiments. Improper preparation may lead to deviations of the crack from the desired location: in the wood, in the resin, or at the wood-resin interface.

#### RESIN

The adhesive is the component used to bond the joint or composite together. Numerous authors (Shimizu and Okuma 1981; Sasaki et al. 1973; White 1976; White and Green 1980; Ebewe et al. 1979, 1982, 1986b; Gagliano and Frazier 2001) have studied parameters associated with the bond-line, including bond-line thickness and resin penetration (Shimizu and Okuma 1981). Both Sasaki et al. (1973) and Ebewe et al. (1979) have shown that there is an optimum bond-line thickness for fracture toughness. This is evident in the work by Ebewe et al. (1979) that compared the fracture toughness for crack initiation with that for arrest of the same crack over a range of bond-line thicknesses for the hard maple/phenol-resorcinol system, shown in Fig. 7. It should be noted that optimums were found for two very different systems. Sasaki found an optimum of 500  $\mu\text{m}$  for Kauri/epoxy, while Ebewe et al. (1979) found an optimum thickness of 85  $\mu\text{m}$  for maple/phenol-resorcinol. Since the optimum thickness is specific to each wood/resin system, each combination of wood species and resin type should be studied independently. Uniformity of the bond-line thickness and the area coverage are also key parameters as Shimizu and Okuma (1981) found that increased uniformity leads to higher strength bond-lines. For a bond-line to be considered perfectly uniform, a sample from any point along that bond-line will be identical to

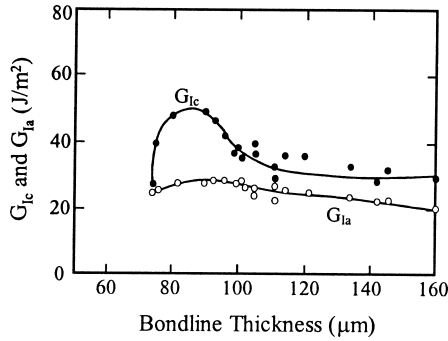


FIG. 7. Effect of bond-line thickness on Mode I fracture toughness for hard maple/phenol-resorcinol system.  $G_{Ic}$  is the critical fracture energy and  $G_{Ia}$  is the arrest load energy. If  $G_{Ic}$  is greater than  $G_{Ia}$  unstable crack growth occurs. (Ebewele et al. 1979)

any other sample taken at a different point. For example, continuous bond-lines will have the same thickness; discontinuous bond-lines will have the same pattern (e.g., droplet spacing and size). In both cases, the bond-line is self-similar along the entire length.

At the wood composites scale, fracture toughness of oriented strandboard is directly affected by the resin dispersion and distribution. These in turn affect the uniformity of the bond-line and the probability of finding sections that are not bonded. The resin dispersion is the size distribution of the resin droplets produced by the atomizer, and resin distribution is the spatial distribution of the resin on the strand. Because of the small amount of adhesive applied in OSB manufacture, on the order of 2 to 3 weight %, the bond-line formed is discontinuous. This leads to stress concentrations at each resin droplet. Kamke et al. (1996) and Youngquist et al. (1987) have demonstrated that the modulus of rupture (MOR) and internal bond (IB) strength increase with an increased uniformity of resin coverage. As well, Kamke et al. (1996) show that a reduction in droplet size also increases the mechanical performance of the OSB. Kamke et al. (1996) have also stated that the optimum dispersion and distribution are unknown.

If a resin droplet is too small, it may be completely absorbed into the strands, leaving

no resin at the interface and available for bonding. Kamke et al. (1996) noted the phenomena in their studies of OSB. This also leads to the sharp decrease in toughness at thin bond-lines as seen in Fig. 7. Joint starvation due to over penetration of resin into the wood will result in reduced mechanical properties. However, some penetration is necessary to repair the adherend surface from damage caused during preparation. This is shown by White (1976), who found that the fracture toughness increased as the penetration depth of the resin into the wood increased. In contrast, Ebewele et al. (1986b) state that a shallow penetration depth can produce weak bonds, but at this time one cannot make a definitive statement on the correlation between penetration depth and mechanical properties.

The effect of resin amount was also studied by Higgins (1990), who used a modified Hankinson equation, similar to Barnes (2001), Eqs. (1) and (2), to model the strength (MOR) of oriented strand composites. In this case, the modification is the use of a von Mises probability distribution function (pdf),  $g(\theta, m, k)$ , to account for the orientation of the strands. Inputs to the model are the concentration parameter,  $k$ , which defines the degree of orientation of the board; the specific longitudinal,  $L$ ; and transverse,  $T$ , tensile strengths of the strands, Eqs. (11) to (13). As the concentration parameter increases, the von Mises pdf narrows and the maximum value increases meaning that a higher proportion of the strands are oriented parallel to the board axis.

$$g(\theta, m, k) = \frac{1}{\pi I_o(k)} e^{k \cos 2(\theta - m)}, \quad (11)$$

$$s(\theta) = \frac{\bar{\sigma}_{\parallel}}{1 + [(\bar{\sigma}_{\parallel}/\bar{\sigma}_{\perp}) - 1] \sin^2 \theta}, \quad (12)$$

$$S_m(\theta) = \int_{-\pi/2}^{\pi/2} g(m, k, \theta) \cdot s(\theta) d\theta, \quad (13)$$

where  $g(\theta, m, k)$  is the grain angle pdf,  $\theta$ , the individual strand grain angle, with respect to the board axis,  $m$ , the angle between the prin-

cipal orientation axis and the axis of load,  $k$ , the orientation parameter of strand angular spread,  $I_0(k)$ , a modified Bessel function of order zero,  $S_m(\theta)$ , a mathematical expectation of composite strength,  $s(\theta)$ , a Hankinson expression for the specific strength of a strand loaded at angle  $\theta$  with respect to its grain,  $\bar{\sigma}_{\parallel}$ , the mean specific tensile strength of strands tested parallel to grain, and  $\bar{\sigma}_{\perp}$ , the mean specific tensile strength of strands tested perpendicular to grain.

Higgins concluded that the model is accurate when sufficient resin is available to provide adequate stress transfer, and underlines the importance of the bond-line in achieving the maximum strength of oriented wood composites. Bonding was increasingly critical as the orientation level, the percentage of strands oriented in the direction of applied load, increased. Experimentally, 5 to 7 times the amount of resin typically used in industry was required to achieve the maximum specific tensile strength predicted by the model. As well, Higgins also found that the internal bond strength of randomly oriented board was reduced by 25% to 30% when as little as 10% of the surface was inadequately covered with resin. In addition, the model put forth by Barnes, Eqs. (1) and (2), also predicts increasing stiffness and strength with increasing strength perpendicular to the bond-line, and emphasizes the significance of the bond-line.

It should be remembered that wood-adhesive joints and wood composites are used for long periods of time, and thus time effects associated with the effectiveness of the bond-line are of importance. River et al. (1989) found that the fracture toughness of UF resins changed with time. Material may initially exhibit stable fracture and have a constant fracture toughness, and at longer times, up to 2 weeks after bonding, the fracture toughness of the adhesive joint can continue to increase. River et al. speculate that this is due to continued cross-linking and physical aging of the resin. This concept of optimum time can also be applied to the curing of a bond-line. Both Gagliano and Frazier (2001) and Ebewele et

al. (1982) found that there is an optimum cure time for maximum fracture toughness. Again, each system has its unique optimum, dependent on the parameters used to form the joint including the substrate, resin, and formation temperature. Gagliano and Frazier report that maximum fracture toughness for the yellow poplar/phenolformaldehyde combination was achieved at a temperature of 175°C after 20 min, whereas Ebewele et al. (1982) reports maximums reached after 30 min to 4 h as the bonding temperature decreases from 150°C to 50°C for the hard maple/phenol-resorcinol system. Both also show a reduction in fracture toughness beyond this optimum time, which they speculated is the result of embrittlement due to excessive cross-linking.

The effect of the bond-line on wood-adhesive joints and wood composites can be summarized as follows. Wood-adhesive joints with the greatest fracture toughness are theoretically those with a uniform thickness of resin: optimum thickness depends on the wood-adhesive combination used. Care should be taken so that overpenetration of the resin into the wood does not occur. This is a concern both for continuous and discontinuous bond-lines. In the case of discontinuous bond-lines, the resin distribution should be uniform and composed of small resin droplets. However, the optimum distribution has not been determined. While work by Barnes and Higgins demonstrates the importance of the bond-line in achieving the desired macroscopic board properties, none of the proposed models addresses how the adhesive bond is affected by resin dispersion and distribution. Therefore, an examination of the effect of resin dispersion and distribution (size variability and inter-droplet spacing) on the fracture toughness of wood-adhesive joints and wood composites would be beneficial.

#### SUMMARY AND CONCLUSIONS

This paper reviews the literature of fracture of wood composites and relates it to fracture of wood-adhesive joints and solid wood. The

review is not exhaustive and literature has been omitted for the sake of brevity. Based purely on geometrical considerations, the literature shows that the basics of structural bonded joint behavior are readily applicable to wood-adhesive joints and wood composites. Strength of both increases with increasing lap length and increasing slenderness ratio (i.e., decreasing lamination or veneer thickness). Fracture mechanics is also applicable to wood composites since the models proposed are based on the concept of intrinsic flaws within the product.

Behavior of the adherends is important. All-wood component sizes: lumber, veneer, strands, particles, and fibers have been studied; and the majority of researchers have concluded that fracture of wood-adhesive joints should occur in wood alone and not at the wood-resin interface for optimum performance. Thus, an understanding of the fracture of solid wood at all levels is also essential to better comprehend the behavior of wood composites. The location of fracture in a wood composite is dependent upon the surface preparation and grain angle of the wood substrates. For OSB in particular, fracture toughness can be improved by improving strand generation. Improved strand generation leads to decreased surface roughness and therefore, as is the case with wood adhesive joints, increased fracture toughness.

Fracture toughness of OSB also increases with increasing uniformity of resin distribution (spatial variability) and decreasing resin dispersion (size variability). Both will lead to greater bond-line uniformity and will increase the fracture toughness, as found in wood-adhesive joints. Despite this knowledge on resin dispersion and distribution, optimum conditions will depend on the wood species and resin system used. In addition, there are currently no proposed models that address the effect of resin dispersion and distribution on the adhesive bond, such models are necessary to optimize the desired macroscopic board properties.

#### ACKNOWLEDGMENTS

The authors would like to thank and acknowledge Forintek Canada Corporation, the Structural Board Association, and the National Science and Engineering Research Council of Canada Collaborative Research and Development Grant Program for providing the financial support for this work.

#### REFERENCES

- AMERICAN SOCIETY FOR TESTING AND MATERIALS (ASTM). 2000. Standard practice for estimating the percentage of wood failure in adhesive bonded joints. Annual Book of ASTM Standards. D5266-99, 15.06, 438–440.
- BARNES, D. 2000. An integrated model of the effect of processing parameters on the strength properties of oriented strand wood products. *Forest Prod. J.* 50(11/12): 33–42.
- . 2001. A model of the effect of strand length and strand thickness on the strength properties of oriented wood composites. *Forest Prod. J.* 51(2):36–45.
- CONRAD, M. P. C., G. FERNLUND, G. D. SMITH, AND R. KNUDSON. 2000. Identification of key parameters for the blending dynamics of OSB: Literature review and preliminary experimentation. Forintek Canada Corp., Vancouver, BC, Canada. 18 pp.
- EBEWELE, R. O., B. H. RIVER, AND J. A. KOUTSKY. 1979. Tapered double cantilever beam fracture tests of phenolic-wood adhesive joints. Part I: Development of specimen geometry; effects of bondline thickness, wood anisotropy, and cure time on fracture energy. *Wood Fiber* 11(3):197–213.
- , ———, AND ———. 1980. Tapered double cantilever beam fracture tests of phenolic-wood adhesive joints. Part II: Effects of surface roughness, the nature of surface roughness, and surface aging on joint fracture energy. *Wood Fiber* 12(1):40–65.
- , ———, AND ———. 1982. Relationship between phenolic adhesive chemistry, cure and joint performance: Effects of base resin constitution and hardener on fracture energy and thermal effects during cure. *J. Adhesion* 14:189–217.
- , ———, AND ———. 1986a. Wood processing variables and adhesive joint performance. *J. Appl. Polym. Sci.* 32:2979–2988.
- , ———, AND ———. 1986b. Relationship between phenolic adhesive chemistry and adhesive joint performance: Effect of filler type on fracture energy. *J. Appl. Polym. Sci.* 31(7/8):2275–2302.
- FURUNO, T., C.-Y. HSE, AND W. A. CÔTÉ. 1983. Observation of microscopic factors affecting strength and dimensional properties of hardwood flakeboard. Pages 297–312 in *Proc. 17th International Particleboard Symposium*, Washington State University, Pullman, WA.



- GAGLIANO, J. M., AND C. E. FRAZIER. 2001. Improvements in the fracture cleavage testing of adhesively-bonded wood. *Wood Fiber Sci.* 33(3):377–385.
- HERTZBERG, R. W. 1996. Deformation and fracture mechanics of engineering materials. John Wiley & Sons, Inc., Toronto, Canada. 786 pp.
- HIGGINS, E. D. 1990. Strength of wood strand composites. Ph.D. Thesis, University of British Columbia, Vancouver, BC, Canada.
- ILCEWICZ, L. B., AND J. B. WILSON. 1981. Fracture mechanics of particleboard using nonlocal theory. *Wood Science* 14(2):65–72.
- JUNG, J., AND J. F. MURPHY. 1983. An investigation of the fracture of butt joints in parallel-laminated veneer. *Wood Fiber Sci.* 15(2):116–134.
- KAMKE, F. E., E. KULTIKOVA, AND C. A. LENTH. 1996. OSB properties as affected by resin distribution. Pages 147–154 in *Proc. Fourth International Panel and Engineered-Wood Technology Conference and Exhibition*.
- KOMATSU, K. 1984. Application of fracture mechanics to the strength of cross-lapped glued timber joints. *Forest Research Institute Bulletin No. 61*. Forest Research Institute, New Zealand Forest Service, Rotorua, New Zealand.
- , H. SASAKI, AND T. MAKU. 1976. Application of fracture mechanics to strength analysis of glued lap joints. *Wood Research: Bull. Wood Research Institute, Kyoto University* 61:11–24.
- LAUFENBERG, T. L. 1984. Flakeboard fracture surface observations and correlation with orthotropic failure criteria. *J. Inst. Wood Science* 10(2):57–65.
- LEI, Y. -K., AND J. B. WILSON. 1979. Fracture toughness of parallel-laminated veneer. *Forest Prod. J.* 29(8):28–32.
- , AND ———. 1980. Fracture toughness of oriented flakeboard. *Wood Science* 12(3):154–161.
- , AND ———. 1981. A model for predicting fracture toughness of flakeboard. *Wood Science* 13(3):151–156.
- LEICESTER, R. H. 1973. Effect of size on the strength of structures. Pages 1–13 in *Forest Products Laboratory, Division of Building Research Technological Paper No. 71*. Commonwealth Scientific and Industrial Research Organization (CSIRO). Melbourne, Australia.
- , AND P. C. BUNKER. 1969. Fracture at butt joints in laminated pine. *Forest Prod. J.* 19(2):59–60.
- , 1974. Applications of linear fracture mechanics in the design of timber structures. Pages 156–164 in *Proc. 23rd Conference of the Australian Fracture Group*. Melbourne, Australia.
- MIHASHI, H., AND M. HOSHINO. 1989. Fracture toughness and tension softening properties of glued laminated timbers. Pages 799–804 in *8th European Conference on Fracture: Fracture Behaviour and Design of Materials and Structures*.
- MIJOVIC, J. S., AND J. A. KOUTSKY. 1979. Effect of wood grain angle on fracture properties and fracture morphology of wood-epoxy joints. *Wood Science* 11(3):164–168.
- MURPHY, J. F. 1986. Strength and stiffness reduction of large notched beams. *J. Struct. Eng.* 112(9):1989–2000.
- RIVER, B. H., AND E. H. OKKONEN. 1993. Contoured wood double cantilever beam specimen for adhesive joint fracture tests. *J. Testing Eval.* 21(1):21–28.
- , T. C. SCOTT, AND J. A. KOUTSKY. 1989. Adhesive joint fracture behavior during setting and aging. *Forest Prod. J.* 39(11/12):23–28.
- SASAKI, H., E. MCARTHUR, AND J. W. GOTTSTEIN. 1973. Maximum strength of end-grain to end-grain butt joints. *Forest Prod. J.* 23(2):48–54.
- SATO, K. 1988a. Influences of specimen size, crack length, loading rate and notch acuity on medium density fiberboard. *J. Japan Wood Research Society* 34(11):955–958.
- . 1988b. Fracture of medium-density fiberboard under mixed mode loading. *J. Japan Wood Research Society* 34(10):828–833.
- SCHNIEWIND, A. P., AND D. E. LYON. 1973. A fracture mechanics approach to the tensile strength perpendicular to grain of dimension lumber. *Wood Sci. Technol.* 7:45–59.
- SCOTT, T. C., B. H. RIVER, AND J. A. KOUTSKY. 1992. Fracture testing wood adhesives with composite cantilever beams. *J. Testing Eval.* 20(4):259–264.
- SHIMIZU, S., AND M. OKUMA. 1981. Fundamental studies on the strength of the oriented particleboard: On the bonding strength between wood particles. *Mokuzai Gakkaishi* 27(1):8–13.
- SIMPSON, W. T. 1977. Model for tensile strength of oriented flakeboard. *Wood Science* 10(2):68–71.
- SMITH, F. W., AND D. T. PENNEY. 1980. Fracture mechanics analysis of butt joints in laminated wood beams. *Wood Science* 12(4):227–235.
- TONG, L., AND G. P. STEVEN. 1999. Analysis and design of structural bonded joints. Kluwer Academic Publishers, Norwell, MA. 288 pp.
- WALSH, P. F., R. H. LEICESTER, AND A. RYAN. 1973. The strength of glued lap joints in timber. *Forest Prod. J.* 23(5):30–33.
- WHITE, M. S. 1976. Influence of resin penetration on the fracture toughness of wood adhesive bonds. *Wood Science* 10(1):6–14.
- , AND D. W. GREEN. 1980. Effect of substrate on the fracture toughness of wood-adhesive bonds. *Wood Science* 12(3):149–153.
- YOUNGQUIST, J. A., G. C. MYERS, AND L. L. MURMANIS. 1987. Resin distribution in hardboard: Evaluated by internal bond strength and fluorescence microscopy. *Wood Fiber Sci.* 19(2):215–224.